Brief Communication

Cell Chemical Biology

Eradicating Bacterial Persisters with Combinations of Strongly and Weakly Metabolism-Dependent Antibiotics

Graphical Abstract

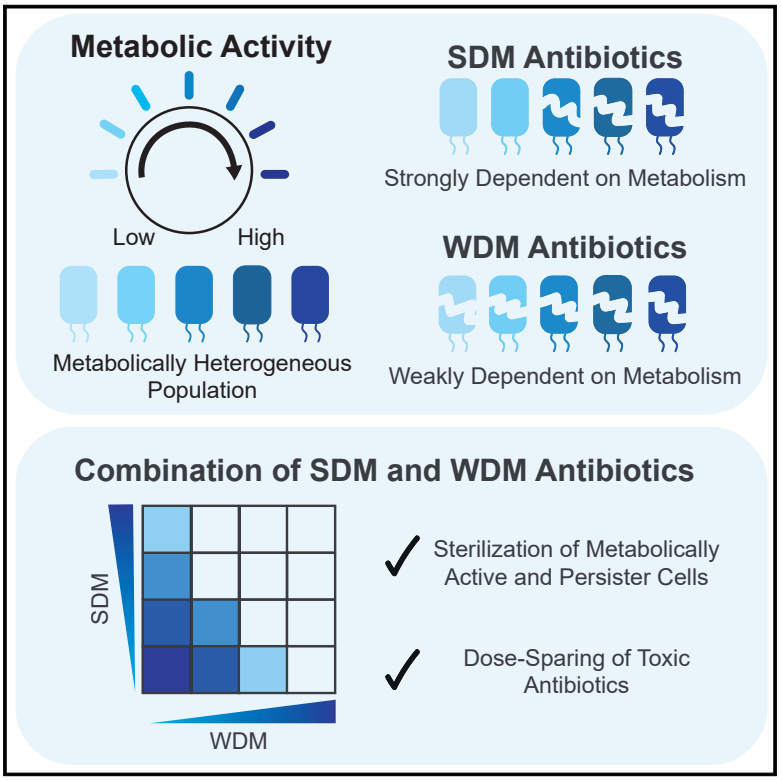

Highlights

- Antibiotics are strongly or weakly dependent on metabolism (SDM or WDM)
- Combinations of SDM and WDM antibiotics sterilize bacteria, while dose-sparing
- SDM and WDM drug interactions are undetectable in growth-inhibition assays

Authors

Erica J. Zheng, Jonathan M. Stokes, James J. Collins

Correspondence

stokesjm@mit.edu (J.M.S.), jimjc@mit.edu (J.J.C.)

In Brief

Zheng et al. rationally combine antibiotics using insights on bacterial metabolism to identify drug-drug combinations that sterilize bacterial cultures of both metabolically active and persister cells, while dose-sparing toxic antibiotics.

Zheng et al., 2020, Cell Chemical Biology *27*, 1544–1552
December 17, 2020
https://doi.org/10.1016/j.chembiol.2020.08.015

CellPress

CellPress
OPEN ACCESS

Cell Chemical Biology

Brief Communication

Eradicating Bacterial Persisters with Combinations of Strongly and Weakly Metabolism-Dependent Antibiotics

Erica J. Zheng,[1,2] Jonathan M. Stokes,[2,3,4,*] and James J. Collins[2,3,5,6,7,*]
[1]Program in Chemical Biology, Harvard University, Cambridge, MA 02138, USA
[2]Broad Institute of MIT and Harvard, Cambridge, MA 02142, USA
[3]Institute for Medical Engineering & Science, Department of Biological Engineering, and Synthetic Biology Center, Massachusetts Institute of Technology, Cambridge, MA 02139, USA
[4]Machine Learning for Pharmaceutical Discovery and Synthesis Consortium, Massachusetts Institute of Technology, Cambridge, MA 02139, USA
[5]Wyss Institute for Biologically Inspired Engineering, Harvard University, Boston, MA 02115, USA
[6]Harvard-MIT Program in Health Sciences and Technology, Cambridge, MA 02139, USA
[7]Lead Contact
*Correspondence: stokesjm@mit.edu (J.M.S.), jimjc@mit.edu (J.J.C.)
https://doi.org/10.1016/j.chembiol.2020.08.015

SUMMARY

The vast majority of bactericidal antibiotics display poor efficacy against bacterial persisters, cells that are in a metabolically repressed state. Molecules that retain their bactericidal functions against such bacteria often display toxicity to human cells, which limits treatment options for infections caused by persisters. Here, we leverage insight into metabolism-dependent bactericidal antibiotic efficacy to design antibiotic combinations that sterilize both metabolically active and persister cells, while minimizing the antibiotic concentrations required. These rationally designed antibiotic combinations have the potential to improve treatments for chronic and recurrent infections.

INTRODUCTION

Bacterial persisters are subpopulations of cells that survive bactericidal antibiotic treatment, despite lacking genetically encoded antibiotic resistance determinants (Lewis, 2010). These persister cells have been associated with chronic and recurrent infections and, in the absence of their sterilization, can re-establish infection upon cessation of antibiotic treatment (Grant and Hung, 2013; Mulcahy et al., 2010). This often necessitates repeated antibiotic treatments that can last, in extreme cases, for years (Grant and Hung, 2013). Indeed, such chronic infections are often caused by *Mycobacterium tuberculosis* and *Pseudomonas aeruginosa*, which cause lung infections, and *Escherichia coli* in the context of urinary tract infections (Grant and Hung, 2013; Mulcahy et al., 2010).

Persisters are metabolically repressed, which protects these cells from killing by most classes of bactericidal antibiotics (Balaban et al., 2004; Shah et al., 2006; Prax and Bertram, 2014). Indeed, it is well established that antibiotic efficacy is strongly dependent on bacterial metabolic state (Lopatkin et al., 2019; Stokes et al., 2019a). This has been extensively shown for the β-lactam, quinolone, and aminoglycoside antibiotic classes using an array of genetic and chemical perturbations of metabolism (Lopatkin et al., 2019; Lobritz et al., 2015; Gutierrez et al., 2017). Furthermore, it has been demonstrated that the efficacy of such antibiotics against bacterial persisters necessitates co-administration of carbon sources for metabolic activation (Allison et al., 2011; Meylan et al., 2018). Interestingly, however, there are examples of molecules not within these common classes that retain bactericidal efficacy against metabolically repressed cells, suggesting that functionally discrete bactericidal antibiotics have varying metabolic requirements for bacterial cell killing (McCall et al., 2019; Grassi et al., 2017; Kwan et al., 2015; Chowdhury et al., 2016; Eng et al., 1991; Conlon et al., 2013; Defraine et al., 2018). Examples of compounds that retain bactericidal efficacy against persister cells include colistin (McCall et al., 2019; Grassi et al., 2017) and the DNA cross-linking anticancer drug mitomycin C (Kwan et al., 2015).

These compounds are promising candidates for treating chronic and recurrent infections due to their ability to eradicate bacteria in diverse metabolic states. However, toxicity to human cells has limited the widespread use of these molecules in the clinic. Indeed, previous work has shown that 65%–85% of patients receiving colistin at plasma concentrations higher than 2.2 μg/mL exhibit signs of nephrotoxicity (Sorlí et al., 2013, 2017). Although the clinical use of colistin was limited beginning in the 1970s in favor of less toxic options, the high prevalence of antibiotic-resistant Gram-negative pathogens has forced the reintroduction of colistin for specific clinical applications in recent years, despite its unfavorable toxicity profile (Poirel et al., 2017).

CellPress
OPEN ACCESS

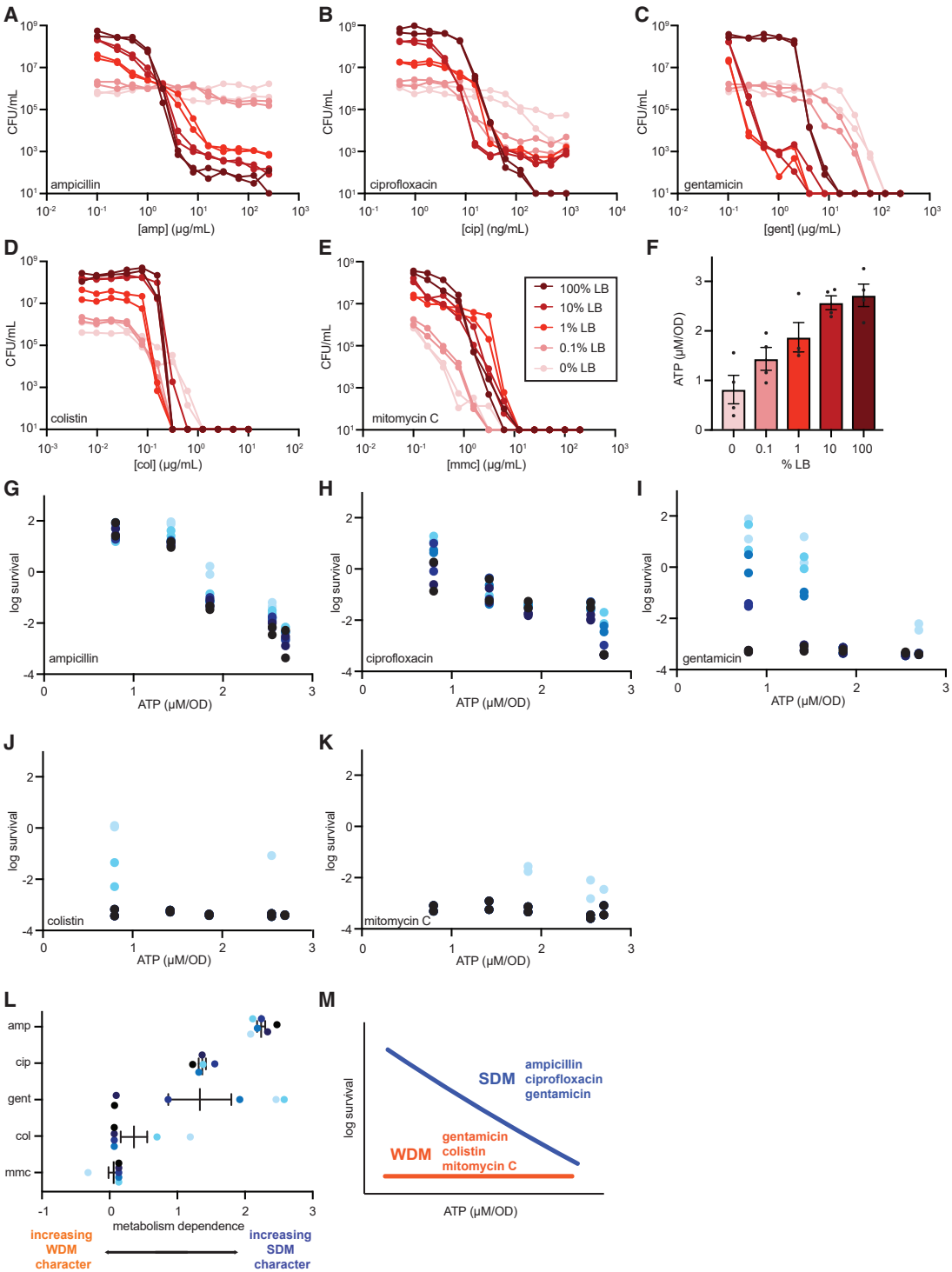

Figure 1. Strongly Dependent on Metabolism (SDM) and Weakly Dependent on Metabolism (WDM) as Descriptors of Bactericidal Antibiotic Efficacy under Diverse Metabolic States

(A–E) Killing of *E. coli* in 0%, 0.1%, 1%, 10%, or 100% LB in PBS for 3 h in biological duplicates. Light to dark shading indicates increasing medium richness. (A) Ampicillin, (B) ciprofloxacin, (C) gentamicin, (D) colistin, (E) mitomycin C.

(F) Intracellular ATP concentration as a function of medium richness. Data are representative of four biological replicates; error bars represent SEM.

(G–K) Bacterial survival as a function of intracellular ATP concentration. Killing data from antibiotic concentrations 2× MIC and greater from (A–E) are included. Light to dark shading represents increasing antibiotic concentration. Data are representative of two biological replicates. (G) Ampicillin, (H) ciprofloxacin, (I) gentamicin, (J) colistin, (K) mitomycin C.

(legend continued on next page)

In addition, mitomycin C causes a range of toxicities, including thrombocytopenia and leukocytopenia (Verweij and Pinedo, 1990). Consequently, the widespread use of these compounds to treat bacterial infections is unfavorable, despite their efficacy against metabolically repressed populations.

Safe and effective methods to eradicate bacteria regardless of metabolic state are critically needed. Currently, however, the direct comparison of metabolic dependencies between discrete antibiotic classes is limited by varying experimental conditions across studies (McCall et al., 2019; Grassi et al., 2017; Kwan et al., 2015; Chowdhury et al., 2016; Eng et al., 1991; Conlon et al., 2013). Here, we investigate the metabolic dependencies of various bactericidal antibiotic classes under standardized conditions. We subsequently leverage this insight to rationally design antibiotic combinations that sterilize both metabolically active and persister cells, while simultaneously dose-sparing. These synergistic combinations provide an important proof of concept toward the development of therapies for chronic and recurrent infections, while minimizing toxicity to patients.

RESULTS

Quantification of Metabolism Dependence across Antibiotic Classes

We tested the bactericidal efficacy of functionally diverse antibiotics against *E. coli* BW25113 in an array of nutrient availabilities that modulate metabolic state (Shimizu, 2014; Mok and Brynildsen, 2019) (Figures 1A–1E). We assayed ampicillin, ciprofloxacin, and gentamicin as representative members of the β-lactam, quinolone, and aminoglycoside classes, respectively. In parallel, we tested colistin and mitomycin C as molecules reported to demonstrate bactericidal efficacy against metabolically repressed cells (McCall et al., 2019; Grassi et al., 2017; Kwan et al., 2015). Consistent with previous literature (Lopatkin et al., 2019; Lobritz et al., 2015; Gutierrez et al., 2017; McCall et al., 2019; Grassi et al., 2017; Kwan et al., 2015), ampicillin and ciprofloxacin lost significant bactericidal efficacy against nutrient-depleted cells, whereas colistin and mitomycin C retained this activity. Gentamicin exhibited concentration-dependent bactericidal efficacy against resource-depleted cells; specifically, at concentrations >15× the minimum inhibitory concentration (MIC) (Figure S1A), we observed significant bacterial cell killing under nutrient-depleted conditions (Figure 1C). Importantly, intracellular ATP concentrations correlated with medium richness (Figure 1F), consistent with the notion that the observed antibiotic efficacies were associated with bacterial metabolic state (Lopatkin et al., 2019). We note here that we observed increased gentamicin efficacy at low drug concentrations in 10% and 1% LB relative to 100% LB, which could be partially rescued by supplementation with L-cysteine at a concentration similar to 100% LB (Sezonov et al., 2007) (Figures S2D and S2E). These observations are consistent with the previously reported protective effect of H_2S from aminoglycoside lethality (Shatalin et al., 2011; Luhachack et al., 2019).

Next, across our set of functionally diverse bactericidal antibiotics, we analyzed bacterial cell killing as a function of metabolic state. Employing the relationship between media richness and intracellular ATP concentration, we utilized our cell viability data shown in Figures 1A–1E and plotted survival against intracellular ATP for antibiotic concentrations 2× MIC and greater (Figures 1G–1K). We then performed linear regression on the cell survival/intracellular ATP relationship for each antibiotic, at every concentration, to acquire a measure of metabolism dependence for each molecule (Table S1). We took the negatives of the resultant slopes as the measures of metabolism dependence, such that greater positive values indicate increasing dependence on metabolism. Finally, we averaged these values across concentrations to obtain the mean metabolism dependence for each antibiotic.

Plotting metabolism dependence for our five representative bactericidal antibiotics, we observed unique metabolic dependencies (Figure 1L), based on which we propose two broad definitions that describe antibiotic behavior across metabolic states (Figure 1M). Drugs whose killing has little dependence on intracellular ATP concentration (and therefore metabolic state), such as mitomycin C and colistin, are referred to as weakly dependent on metabolism (WDM). Ampicillin and ciprofloxacin, whose efficacies clearly correlate with bacterial metabolic state, are referred to as strongly dependent on metabolism (SDM). Gentamicin presents an intriguing case, where at lower concentrations SDM behavior is observed, but at higher concentrations WDM behavior is observed. We posit that this concentration-dependent shift in metabolic-dependent bactericidal efficacy is perhaps due to disruption of the cell envelope at higher concentrations, as has been described previously (Bulitta et al., 2015; Martin and Beveridge, 1986).

We note here that while nutrient availability is an effective means through which bacterial metabolic state can be modulated, previous work has shown that treatment of cells with bacteriostatic antibiotics also suppresses metabolic activity (Lobritz et al., 2015; Lin et al., 2014), which inhibits further killing by bactericidal antibiotics from the β-lactam, quinolone, and aminoglycoside classes (Lobritz et al., 2015; McCall et al., 2019). Indeed, we confirmed that a 30-min pre-treatment with the bacteriostatic agent chloramphenicol protected *E. coli* from killing by ampicillin, ciprofloxacin, and gentamicin, but not from colistin and mitomycin C (Figures S2G–S2K), consistent with our observations of bacterial cell killing by these antibiotics in media of varying richness.

Combinations of SDM and WDM Antibiotics Sterilize Bacterial Cultures and Are Dose-Sparing

We hypothesized that the concentration of WDM antibiotic required to sterilize cultures could be reduced by first utilizing an SDM antibiotic to eliminate metabolically active bacteria (Figure 2A, left). Indeed, the goal of such combinations is 2-fold: first, to efficiently sterilize the culture of both active and persister cells, and second, to dose-spare the amount of WDM

(L) Comparing the metabolic dependence of bactericidal antibiotic efficacy. Center bars represent the mean, and individual metabolism dependence values at each antibiotic concentration are shown, with light to dark shading indicating increasing concentration. Error bars represent SEM. Regression statistics (slope and R^2) are shown in Table S1.

(M) Describing antibiotic efficacy in relation to bacterial metabolic state.

CellPress
OPEN ACCESS

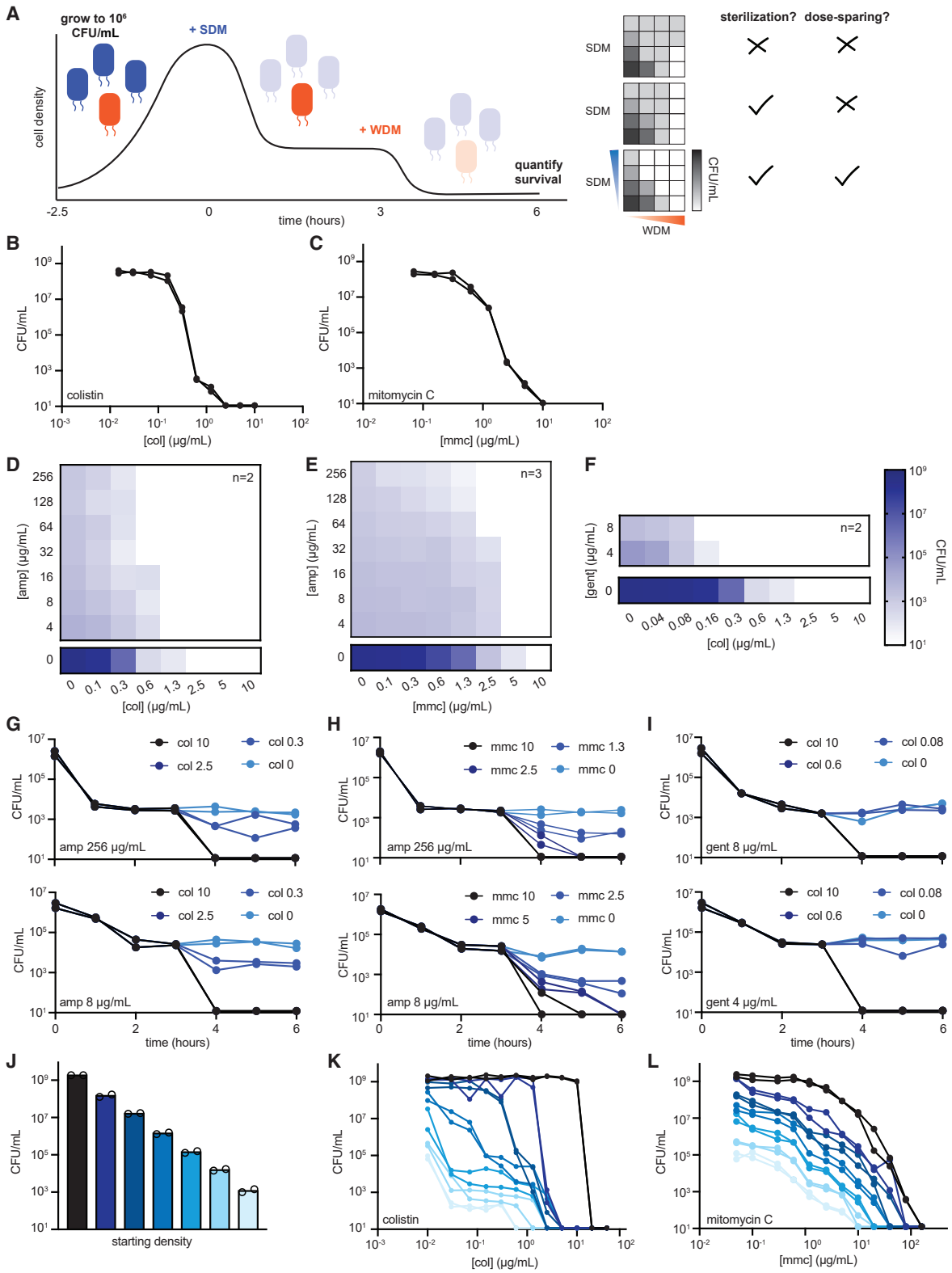

Figure 2. Rational Combinations of SDM and WDM Antibiotics Sterilize Cultures While Dose-Sparing

(A) Schematic of combination treatment. (Left) *E. coli* was grown to ~10^6 CFU/mL and 2-fold serial dilutions of an SDM antibiotic were added for 3 h to eliminate metabolically active cells (blue). Next, 2-fold serial dilutions of a WDM antibiotic were added for an additional 3 h, eradicating remaining persisters (orange). (Right)

(legend continued on next page)

antibiotic—generally, the more toxic molecule—relative to WDM antibiotic monotherapy.

To empirically validate this combination strategy, we first determined the amount of WDM antibiotic needed to sterilize a culture as a single agent. We observed that over a 3-h exposure, 2.5 μg/mL colistin alone, or 10 μg/mL mitomycin C alone, is required to sterilize ~10^6 CFU/mL of *E. coli* in LB medium (Figures 2B and 2C). We next assayed the combination of ampicillin (an SDM antibiotic) and colistin (a WDM antibiotic). Here, cells were treated with 2-fold serial dilutions of ampicillin for 3 h, followed by 2-fold serial dilutions of colistin for an additional 3 h, creating a checkerboard with varied concentrations of both compounds, which were then plated and evaluated for cell survival. In these killing checkerboards, we sought to distinguish between three possible outcomes: (1) loss of sterilization, wherein SDM antibiotic treatment antagonized the activity of WDM antibiotics; (2) sterilization of persisters by the WDM antibiotic in the absence of dose-sparing; or (3) sterilization with dose-sparing of the WDM antibiotic (Figure 2A, right).

We observed that even at 256 μg/mL, ampicillin alone was insufficient to sterilize the culture, leaving 10^3–10^4 CFU/mL persister cells (Figures 2D and S1B). However, the addition of colistin following ampicillin exposure sterilized the persister subpopulation, and the amount of colistin required for sterilization could be reduced 4-fold in combination, indicating successful sterilization with dose-sparing (Figures 2D and S3A). Analysis of killing dynamics of the combination treatment revealed that persisters that survive SDM antibiotic treatment are killed at similar rates by colistin relative to the use of colistin as a monotherapy (Figures 2G and S1B). Importantly, the reduced colistin concentration needed for persister sterilization in the combination regimen is below its EUCAST breakpoint of 2 μg/mL (The European Committee on Antimicrobial Susceptibility Testing, 2020).

Further investigation into this antibiotic combination strategy revealed additional combinations of SDM and WDM antibiotics that sterilized cultures while simultaneously dose-sparing, such as ampicillin and mitomycin C, with a 4-fold reduction in mitomycin C required for sterilization (Figures 2E, 2H, and S3B), and ciprofloxacin and colistin, with 2-fold dose-sparing for colistin (Figure S3C). Notably, gentamicin (at SDM concentrations) and colistin allowed for a remarkable 16-fold reduction in the concentration of colistin required for sterilization (Figures 2F, 2I, and S3D). Up to 16-fold dose-sparing with colistin was also observed in combination with the aminoglycoside kanamycin (Figures S2A–S2C and S3E), showing the generalizability of the aminoglycoside-colistin dose-sparing. Indeed, for these combinations, sterilization of persisters could be achieved near the MIC of colistin and far below the clinical breakpoint concentration. Taken together, these data suggest that combinations of SDM and WDM antibiotics allow for the sterilization of both metabolically active cells and persister cells, while dose-sparing the commonly more toxic WDM antibiotic.

We posit that the mechanism of the observed WDM antibiotic dose-sparing can be attributed to the correlation of WDM antibiotic bactericidal potency with culture density. Indeed, lower concentrations of WDM antibiotic are required to sterilize cultures of lower density (Figures 2J–2L). Therefore, first eliminating the majority of metabolically active cells with an SDM antibiotic lowers the concentration of WDM antibiotic required for sterilization. However, it should be noted that this density dependence does not account for the enhanced dose-sparing between aminoglycosides and colistin, compared with ampicillin and ciprofloxacin in combination with colistin, as initial treatment by all SDM antibiotics tested herein resulted in similar persister fractions. It is possible that the additional dose-sparing observed between aminoglycosides and colistin may be due to the effect of non-lethal damage on the cell envelope inflicted by aminoglycosides that renders bacteria more vulnerable to colistin lethality and acts synergistically with colistin-mediated destabilization of the outer membrane. Further work is needed to elucidate the precise mechanism of the enhanced aminoglycoside-colistin dose-sparing.

WDM Antibiotics Are Required for Sterilization of Persister Cells

To test whether the observed dose-sparing and culture sterilization were specific to the combination of SDM antibiotics followed by WDM antibiotics, we treated *E. coli* with ampicillin followed by ciprofloxacin, two SDM antibiotics. Ciprofloxacin failed to sterilize the persister subpopulation remaining after ampicillin exposure, suggesting that WDM antibiotics are required for sterilization (Figures 3A and S3F). Indeed, this was also observed with the combination of ciprofloxacin followed by ampicillin, in which ampicillin was ineffective against the persister subpopulation remaining after ciprofloxacin exposure (Figures 3B and S3G). Interestingly, we observed that gentamicin exhibited minimal, but detectable, activity against ampicillin and ciprofloxacin persisters even at concentrations at which its behavior would be considered SDM-like as a monotherapy, highlighting the dual SDM/WDM nature of aminoglycosides that is dependent on both drug concentration and culture conditions (Figures 3C, 3D, S3H, and S3I).

Combinations were evaluated for both culture sterilization and dose-sparing. Three possible outcomes are depicted. Darker boxes in model checkerboards represent areas of higher cell density.

(B and C) Sterilization of cultures by WDM antibiotics alone. *E. coli* was grown to ~10^6 CFU/mL, then colistin (B) or mitomycin C (C) was added for 3 h. Data are representative of two biological replicates.

(D–F) Bacterial cell killing checkerboard assays conducted as described in (A) using ampicillin and colistin (D), ampicillin and mitomycin C (E), and gentamicin and colistin (F). Data from (B) or (C) are displayed as a heatmap below each checkerboard for evaluation of dose-sparing efficacy. Data are representative of at least two biological replicates. Individual replicates are shown in Figure S3. Darker boxes represent higher survival. Culture density scale is shown at the right.

(G–I) Kinetic analysis of combination treatment for ampicillin and colistin (G), ampicillin and mitomycin C (H), and gentamicin and colistin (I). Legends show the concentration of WDM antibiotics added in μg/mL at t = 3 h. Data are representative of two biological replicates.

(J–L) Density dependence of WDM antibiotics. Overnight cultures of *E. coli* were serially diluted 10-fold to create a gradient of cell densities (J), then colistin (K) or mitomycin C (L) was added for 3 h. Data are representative of two biological replicates. Shading in (K) and (L) matches cell densities displayed in (J), with light to dark shading indicating increasing initial cell density.

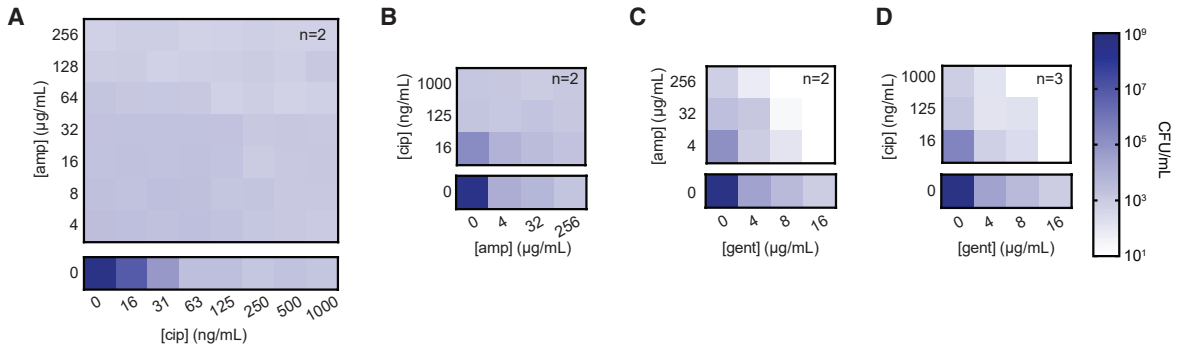

Figure 3. Sterilization of Persister Cells Requires Addition of WDM Antibiotics

Killing checkerboard assays with combinations of ampicillin and ciprofloxacin (A), ciprofloxacin and ampicillin (B), ampicillin and gentamicin (C), and ciprofloxacin and gentamicin (D). Killing data of ~10^6 CFU/mL by the second antibiotic over 3 h are shown below each checkerboard. Data are representative of at least two biological replicates. Individual replicates are shown in Figure S3. Culture density scale is shown at the right.

Interactions between SDM and WDM Antibiotics Are Undetectable in Conventional Growth-Inhibition Assays

The chemical-chemical interactions between two antibiotics are conventionally assessed using growth-inhibition checkerboard assays (Tyers and Wright, 2019). However, growth inhibition does not inform on antibiotic efficacy as defined by bacterial cell death, particularly under the nutrient-depleted conditions considered in this study, where bacterial population expansion is not possible (Traczewski et al., 2009; Brauner et al., 2016). Nonetheless, to determine whether interactions could be detected between SDM and WDM antibiotics using conventional growth-inhibition checkerboard approaches, we performed these assays and calculated fractional inhibitory concentration indices (FICIs) for each antibiotic combination. Indeed, the dose-sparing effects observed in our bacterial cell-killing checkerboards are absent in growth-inhibition checkerboards, with FICIs ranging between 1 and 2 (Tyers and Wright, 2019) (Figures 4A–4C and S4). The absence of any observable interactions in the context of growth inhibition highlights the fact that these assays limit the detection of viability-based phenotypes that are relevant to infection settings, such as the roles of population heterogeneity and metabolic state in antibiotic efficacy (Meylan et al., 2018; Cornforth et al., 2018).

We note here that colistin is well known to potentiate high-molecular-weight and hydrophobic antibiotics under growth-inhibition conditions due to its ability to disrupt and permeabilize the Gram-negative cell envelope (Gordon et al., 2010; Brennan-Krohn et al., 2018; MacNair et al., 2018). Importantly, because we did not observe synergy via growth inhibition between compounds that dose-spare under killing conditions, and given that the compounds that dose-spare with colistin under killing conditions are not large nor have significant hydrophobic properties, it is unlikely that the interactions we observe in this context are attributed simply to increased antibiotic permeability into the cell. Moreover, mitomycin C is not known to damage the bacterial cell membrane, yet dose-sparing was seen in killing checkerboards when used in combination with ampicillin, further supporting the notion that our observations are not simply the result of enhanced permeability.

Maximum Dose-Sparing of WDM Antibiotics Is Observed in Staggered Killing Checkerboards

Conventional antibiotic checkerboard assays monitoring growth inhibition involve simultaneous addition of both compounds, whereas the combination treatment presented herein staggers the addition of each antibiotic. To examine the effect of sequential antibiotic treatment in killing checkerboards, we administered ampicillin and colistin simultaneously for 3 h. We observed that dose-sparing and sterilization still occurred, although dose-sparing in this context was diminished relative to the staggered addition (Figures 4D and S3J). Simultaneous administration of gentamicin and colistin similarly resulted in less dose-sparing than the staggered administration (Figures 4E and S3K). As expected, no sterilization or dose-sparing was observed when cells were treated simultaneously with two SDM antibiotics, ampicillin and ciprofloxacin (Figures 4F and S3L). Additional work to understand the importance of staggered antibiotic treatment to maximize combination efficacy is warranted.

DISCUSSION

In recent years, the link between metabolically repressed, antibiotic-tolerant bacteria and chronic and recurrent infections has become increasingly evident (Grant and Hung, 2013; Mulcahy et al., 2010; Meylan et al., 2018). The strong metabolism dependence of conventional antibiotics from the β-lactam, quinolone, and aminoglycoside classes significantly limits their efficacy against such recalcitrant infections (Lopatkin et al., 2019; Lobritz et al., 2015; Gutierrez et al., 2017). As a result, there has been growing interest in the discovery of treatments whose efficacy is unaffected by perturbations in metabolic state (Defraine et al., 2018). Here, our assessment of an array of functional classes of bactericidal antibiotics reveals a broad range of metabolic dependencies in the context of bactericidal efficacy. Moreover, our work provides a valuable metric for quantifying these dependencies, which can be widely adopted to evaluate the bactericidal capabilities of compounds in infection-relevant settings.

These differences in metabolic dependencies among bactericidal antibiotics can be harnessed to rationally design effective

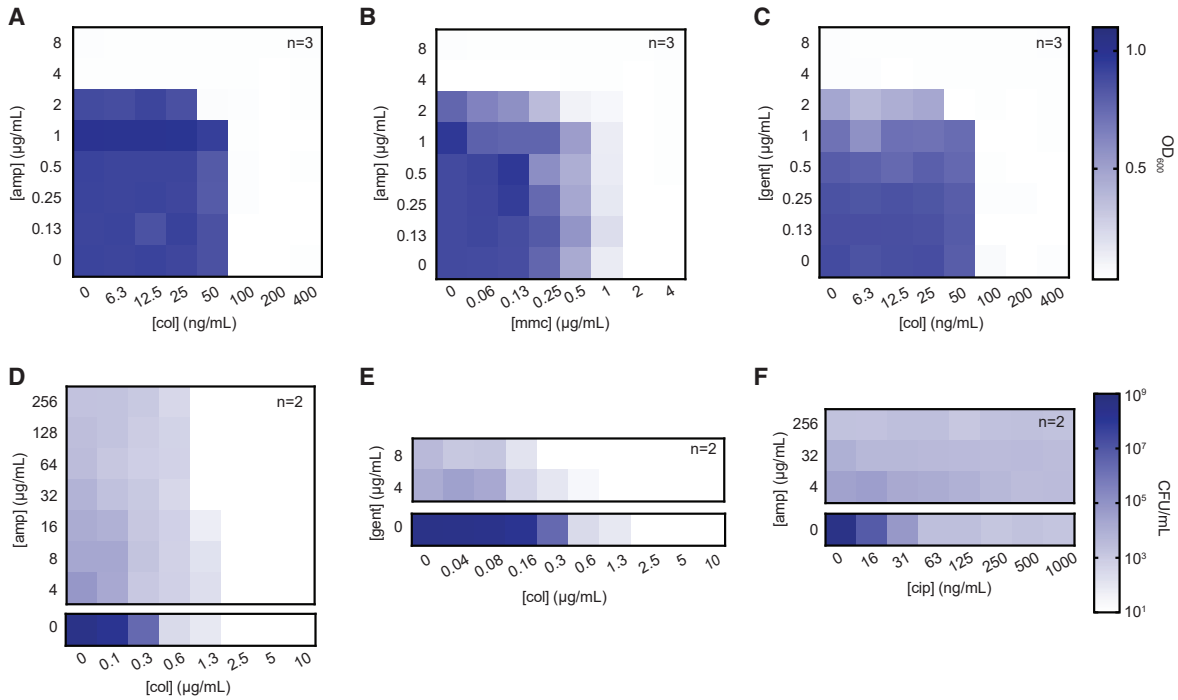

Figure 4. Interactions between SDM and WDM Antibiotics Are Maximized in Staggered Killing Checkerboards

(A–C) Growth-inhibition checkerboards with combinations of ampicillin and colistin (A), ampicillin and mitomycin C (B), and gentamicin and colistin (C). Data are representative of three biological replicates. Individual checkerboard replicates are shown in Figure S4. Darker boxes represent increased optical density. Optical density scale is shown at the far right.

(D–F) Killing checkerboards where both antibiotics are added simultaneously for 3 h. Ampicillin and colistin (D), gentamicin and colistin (E), and ampicillin and ciprofloxacin (F) combinations are shown. Data are representative of two biological replicates; individual replicates are shown in Figure S3. Cell density scale is shown at the far right.

treatments that take into consideration the diversity of metabolic states present in a clonal culture. Indeed, along with what we show herein, there is precedent for this approach in anti-cancer drug discovery, where metabolic insight has informed the design of drug combinations (Wang et al., 2019; Lee et al., 2019; Kishton and Rathmell, 2015; Pribluda et al., 2015). For instance, cells that tolerate the anti-cancer drug sorafenib have upregulated expression of the glycolytic enzyme HK2, and a combination of sorafenib and 2-deoxy-D-glucose, an inhibitor of HK2, was shown to cause persister cell apoptosis and reduced tumor growth in mice (Wang et al., 2019). Building off these metabolic principles, the discovery of treatments that are effective against bacterial pathogens in infection-relevant settings will likely require assessing metabolic phenotypes beyond conventional growth-based assays and examining lethality in multiple metabolic contexts (Stokes et al., 2019b).

As we continue to use antibiotics in the clinic and increasingly search for antibacterial molecules in the face of heightened antibiotic resistance, an important question to consider is whether WDM antibiotics, simply by virtue of their mechanisms, will inherently cause toxicity to human cells (Hurdle et al., 2011). If this is the case, the use of combination treatments that account for the metabolic heterogeneity of bacterial pathogens, as well as the influence of bacterial metabolic state on antibiotic efficacy, will be essential to allow more tolerable therapies for chronic and recurrent infections.

SIGNIFICANCE

Few bactericidal antibiotics are effective against metabolically repressed bacterial persisters, and those that are cause toxicity to human cells. Our inability to effectively eradicate persisters in the clinic has been linked to chronic and recurrent infections, and as a result there has been growing interest in discovering molecules that retain efficacy against such metabolically repressed cells. Here, we develop a metric for evaluating the metabolic dependencies of various antibiotic classes that can be broadly applied to assess the efficacy of compounds against cells in diverse metabolic states. Moreover, we apply this metabolic insight to design combination treatments that sterilize bacterial cultures, including persister cells, while reducing the amount of toxic antibiotics required. This work demonstrates the utility of a metabolism-focused approach to antibiotic therapy that accounts for the heterogeneity present in bacterial cultures.

STAR★METHODS

Detailed methods are provided in the online version of this paper and include the following:

- KEY RESOURCES TABLE
- RESOURCE AVAILABILITY

SUPPLEMENTAL INFORMATION

Supplemental Information can be found online at https://doi.org/10.1016/j.chembiol.2020.08.015.

ACKNOWLEDGMENTS

We thank Ian Andrews and Felix Wong for input on data interpretation and manuscript editing. This work was supported by the Defense Threat Reduction Agency (HDTRA1-15-1-0051 to J.J.C.), the Broad Institute of MIT and Harvard, the Banting Postdoctoral Fellowships Program (393360 to J.M.S.), and a generous gift from A. and J. Bekenstein.

AUTHOR CONTRIBUTIONS

E.J.Z., J.M.S., and J.J.C. conceptualized the study. E.J.Z. designed and carried out experiments, analyzed and interpreted data, and wrote the manuscript. J.M.S. assisted with data interpretation and manuscript editing. J.J.C. assisted with data interpretation and manuscript editing and acquired funding.

DECLARATION OF INTERESTS

J.J.C. is scientific co-founder and scientific advisory board chair of EnBiotix, an antibiotic drug discovery company.

Received: June 17, 2020
Revised: August 10, 2020
Accepted: August 20, 2020
Published: September 10, 2020

REFERENCES

Allison, K.R., Brynildsen, M.P., and Collins, J.J. (2011). Metabolite-enabled eradication of bacterial persisters by aminoglycosides. Nature *473*, 216–220.

Balaban, N.Q., Merrin, J., Chait, R., Kowalik, L., and Leibler, S. (2004). Bacterial persistence as a phenotypic switch. Science *305*, 1622–1625.

Brauner, A., Fridman, O., Gefen, O., and Balaban, N.Q. (2016). Distinguishing between resistance, tolerance and persistence to antibiotic treatment. Nat. Rev. Microbiol. *14*, 320–330.

Brennan-Krohn, T., Pironti, A., and Kirby, J.E. (2018). Synergistic activity of colistin-containing combinations against colistin-resistant *Enterobacteriaceae*. Antimicrob. Agents Chemother. *62*, e00873–18.

Bulitta, J.B., Ly, N.S., Landersdorfer, C.B., Wanigaratne, N.A., Velkov, T., Yadav, R., Oliver, A., Martin, L., Shin, B.S., Forrest, A., et al. (2015). Two mechanisms of killing of *Pseudomonas aeruginosa* by tobramycin assessed at multiple inocula via mechanism-based modeling. Antimicrob. Agents Chemother. *59*, 2315–2327.

Chowdhury, N., Wood, T.L., Martínez-Vázquez, M., García-Contreras, R., and Wood, T.K. (2016). DNA-crosslinker cisplatin eradicates bacterial persister cells. Biotechnol. Bioeng. *113*, 1984–1992.

Conlon, B.P., Nakayasu, E.S., Fleck, L.E., LaFleur, M.D., Isabella, V.M., Coleman, K., Leonard, S.N., Smith, R.D., Adkins, J.N., and Lewis, K. (2013). Activated ClpP kills persisters and eradicates a chronic biofilm infection. Nature *503*, 365–370.

Cornforth, D.M., Dees, J.L., Ibberson, C.B., Huse, H.K., Mathiesen, I.H., Kirketerp-Møller, K., Wolcott, R.D., Rumbaugh, K.P., Bjarnsholt, T., and Whiteley, M. (2018). *Pseudomonas aeruginosa* transcriptome during human infection. Proc. Natl. Acad. Sci. U S A *115*, E5125–E5134.

Defraine, V., Fauvart, M., and Michiels, J. (2018). Fighting bacterial persistence: current and emerging anti-persister strategies and therapeutics. Drug Resist. Updat. *38*, 12–26.

Eng, R.H.K., Padberg, F.T., Smith, S.M., Tan, E.N., and Cherubin, C.E. (1991). Bactericidal effects of antibiotics on slowly growing and nongrowing bacteria. Antimicrob. Agents Chemother. *35*, 1824–1828.

Gordon, N.C., Png, K., and Wareham, D.W. (2010). Potent synergy and sustained bactericidal activity of a vancomycin-colistin combination versus multidrug-resistant strains of *Acinetobacter baumannii*. Antimicrob. Agents Chemother. *54*, 5316–5322.

Grant, S.S., and Hung, D.T. (2013). Persistent bacterial infections, antibiotic tolerance, and the oxidative stress response. Virulence *4*, 273–283.

Grassi, L., Di Luca, M., Maisetta, G., Rinaldi, A.C., Esin, S., Trampuz, A., and Batoni, G. (2017). Generation of persister cells of *Pseudomonas aeruginosa* and *Staphylococcus aureus* by chemical treatment and evaluation of their susceptibility to membrane-targeting agents. Front. Microbiol. *8*, 1917.

Gutierrez, A., Jain, S., Bhargava, P., Hamblin, M., Lobritz, M.A., and Collins, J.J. (2017). Understanding and sensitizing density-dependent persistence to quinolone antibiotics. Mol. Cell *68*, 1147–1154.

Hurdle, J.G., O'Neill, A.J., Chopra, I., and Lee, R.E. (2011). Targeting bacterial membrane function: an underexploited mechanism for treating persistent infections. Nat. Rev. Microbiol. *9*, 62–75.

Kishton, R.J., and Rathmell, J.C. (2015). Novel therapeutic targets of tumor metabolism. Cancer J. *21*, 62–69.

Kwan, B.W., Chowdhury, N., and Wood, T.K. (2015). Combatting bacterial infections by killing persister cells with mitomycin C. Environ. Microbiol. *17*, 4406–4414.

Lee, H., Oh, Y., Jeon, Y.-J., Lee, S.-Y., Kim, H., Lee, H.-J., and Jung, Y.-K. (2019). DR4-Ser424 O-GlcNAcylation promotes sensitization of TRAIL-tolerant persisters and TRAIL-resistant cancer cells to death. Cancer Res. *79*, 2839–2852.

Lewis, K. (2010). Persister cells. Annu. Rev. Microbiol. *64*, 357–372.

Lin, X., Kang, L., Li, H., and Peng, X. (2014). Fluctuation of multiple metabolic pathways is required for *Escherichia coli* in response to chlortetracycline stress. Mol. Biosyst. *10*, 901–908.

Lobritz, M.A., Belenky, P., Porter, C.B.M., Gutierrez, A., Yang, J.H., Schwarz, E.G., Dwyer, D.J., Khalil, A.S., and Collins, J.J. (2015). Antibiotic efficacy is linked to bacterial cellular respiration. Proc. Natl. Acad. Sci. U S A *112*, 8173–8180.

Lopatkin, A.J., Stokes, J.M., Zheng, E.J., Yang, J.H., Takahashi, M.K., You, L., and Collins, J.J. (2019). Bacterial metabolic state more accurately predicts antibiotic lethality than growth rate. Nat. Microbiol. *4*, 2109–2117.

Luhachack, L., Rasouly, A., Shamovsky, I., and Nudler, E. (2019). Transcription factor YcjW controls the emergency H2S production in *E. coli*. Nat. Commun. *10*, 2868.

MacNair, C.R., Stokes, J.M., Carfrae, L.A., Fiebig-Comyn, A.A., Coombes, B.K., Mulvey, M.R., and Brown, E.D. (2018). Overcoming mcr-1 mediated colistin resistance with colistin in combination with other antibiotics. Nat. Commun. *9*, 458.

Martin, N.L., and Beveridge, T.J. (1986). Gentamicin interaction with *Pseudomonas aeruginosa* cell envelope. Antimicrob. Agents Chemother. *29*, 1079–1087.

McCall, I.C., Shah, N., Govindan, A., Baquero, F., and Levin, B.R. (2019). Antibiotic killing of diversely generated populations of nonreplicating bacteria. Antimicrob. Agents Chemother. *63*, e02360–18.

Meylan, S., Andrews, I.W., and Collins, J.J. (2018). Targeting antibiotic tolerance, pathogen by pathogen. Cell *172*, 1228–1238.

Mok, W.W.K., and Brynildsen, M.P. (2019). Nutrient depletion and bacterial persistence. In Persister Cells and Infectious Disease, K. Lewis, ed. (Springer Nature Switzerland), pp. 99–132.

Mulcahy, L.R., Burns, J.L., Lory, S., and Lewis, K. (2010). Emergence of *Pseudomonas aeruginosa* strains producing high levels of persister cells in patients with cystic fibrosis. J. Bacteriol. *192*, 6191–6199.

Poirel, L., Jayol, A., and Nordmann, P. (2017). Polymyxins: antibacterial activity, susceptibility testing, and resistance mechanisms encoded by plasmids or chromosomes. Clin. Microbiol. Rev. *30*, 557–596.

Prax, M., and Bertram, R. (2014). Metabolic aspects of bacterial persisters. Front. Cell. Infect. Microbol. *4*, 148.

Pribluda, A., de la Cruz, C.C., and Jackson, E.L. (2015). Intratumoral heterogeneity: from diversity comes resistance. Clin. Cancer Res. *21*, 2916–2923.

Sezonov, G., Joseleau-Petit, D., and D'Ari, R. (2007). *Escherichia coli* physiology in Luria-Bertani Broth. J. Bacteriol. *189*, 8746–8749.

Shah, D., Zhang, Z., Khodursky, A.B., Kaldalu, N., Kurg, K., and Lewis, K. (2006). Persisters: a distinct physiological state of *E. coli*. BMC Microbiol. *6*, 53.

Shatalin, K., Shatalina, E., Mironov, A., and Nudler, E. (2011). H_2S: A Universal Defense Against Antibiotics in Bacteria. Science *334*, 986–990.

Shimizu, K. (2014). Regulation systems of bacteria such as *Escherichia coli* in response to nutrient limitation and environmental stresses. Metabolites *4*, 1–35.

Sorlí, L., Luque, S., Grau, S., Berenguer, N., Segura, C., Montero, M.M., Álvarez-Lerma, F., Knobel, H., Benito, N., and Horcajada, J.P. (2013). Trough colistin plasma level is an independent risk factor for nephrotoxicity: a prospective observational cohort study. BMC Infect. Dis. *13*, 380.

Stokes, J.M., Lopatkin, A.J., Lobritz, M.A., and Collins, J.J. (2019a). Bacterial metabolism and antibiotic efficacy. Cell Metab. *30*, 251–259.

Sorlí, L., Luque, S., Segura, C., Campillo, N., Montero, M., Esteve, E., Herrera, S., Benito, N., Alvarez-Lerma, F., Grau, S., et al. (2017). Impact of colistin plasma levels on the clinical outcome of patients with infections caused by extremely drug-resistant *Pseudomonas aeruginosa*. BMC Infect. Dis. *17*, 11.

Stokes, J.M., Gutierrez, A., Lopatkin, A.J., Andrews, I.W., French, S., Matic, I., Brown, E.D., and Collins, J.J. (2019b). A multiplexable assay for screening antibiotic lethality against drug-tolerant bacteria. Nat. Methods *16*, 303–306.

The European Committee on Antimicrobial Susceptibility Testing (2020). Breakpoint tables for interpretation of MICs and zone diameters. Version 10.0. http://www.eucast.org.

Traczewski, M.M., Katz, B.D., Steenbergen, J.N., and Brown, S.D. (2009). Inhibitory and bactericidal activities of daptomycin, vancomycin, and teicoplanin against methicillin-resistant *Staphylococcus aureus* isolates collected from 1985 to 2007. Antimicrob. Agents Chemother. *53*, 1735–1738.

Tyers, M., and Wright, G.D. (2019). Drug combinations: a strategy to extend the life of antibiotics in the 21st century. Nat. Rev. Microbiol. *17*, 141–155.

Verweij, J., and Pinedo, H.M. (1990). Mitomycin C: mechanism of action, usefulness and limitations. Anticancer Drugs *1*, 5–13.

Wang, L., Yang, Q., Peng, S., and Liu, X. (2019). The combination of the glycolysis inhibitor 2-DG and sorafenib can be effective against sorafenib-tolerant persister cancer cells. Onco Targets Ther. *12*, 5359–5373.

CellPress
OPEN ACCESS

STAR★METHODS

KEY RESOURCES TABLE

REAGENT or RESOURCE	SOURCE	IDENTIFIER
Bacterial and Virus Strains		
Escherichia coli BW25113	CGSC	CGSC# 7636
Chemicals, Peptides, and Recombinant Proteins		
Ampicillin sodium salt	Sigma-Aldrich	Cat# A0166
Ciprofloxacin	Sigma-Aldrich	Cat# 17850
Gentamicin sulfate salt	Sigma-Aldrich	Cat# G1264
Kanamycin sulfate	Sigma-Aldrich	Cat# 60615
Colistin sulfate salt	Sigma-Aldrich	Cat# C4461
Mitomycin C	Cayman Chemical	Cat# 11435
Chloramphenicol	Sigma-Aldrich	Cat# C0378
L-cysteine	Sigma-Aldrich	Cat# C7352
L-alanine	Sigma-Aldrich	Cat# A7469
Adenosine 5′-triphosphate disodium salt hydrate	Sigma-Aldrich	Cat# A2383
Critical Commercial Assays		
BacTiter-Glo Microbial Cell Viability Assay	Promega	Cat# G8230
Software and Algorithms		
Prism 8	Graphpad	https://www.graphpad.com/scientific-software/prism/

RESOURCE AVAILABILITY

Lead Contact

Further information and requests for resources and reagents should be directed to James J. Collins (jimjc@mit.edu).

Materials Availability

This study did not generate new unique reagents.

Data and Code Availability

This study did not generate new code. Data supporting this study are available from the lead contact upon request.

EXPERIMENTAL MODEL AND SUBJECT DETAILS

E. coli BW25113 was used as the experimental model for all experiments. Experiments were conducted at 37°C as described.

METHOD DETAILS

Antibiotic Efficacy in Varied Nutrient Levels

Single colonies of *E. coli* BW25113 were picked from solid Luria-Bertani (LB) agar, inoculated into 3 mL of liquid LB, and grown overnight at 37°C with 300 r.p.m. shaking. Overnight cultures were diluted 1 in 10,000 into 25 mL of LB and sub-cultured at 37°C with 300 r.p.m. shaking until OD_{600} reached 0.1-0.2 (~4 hours), then centrifuged at 4000 x g for 15 minutes at 4°C. The cell pellet was washed three times with ice-cold phosphate buffered saline (PBS), and nutrient-limited conditions were created by re-suspending cells in 0, 0.1, 1, 10, or 100% LB in PBS, then incubating for two hours at 37°C with 300 r.p.m. shaking. All cultures were then back-diluted in their respective nutrient conditions to an OD_{600} of 0.01 (~10^6 CFU/mL) to normalize cell density across nutrient conditions at the time of antibiotic addition. An aliquot of cells was taken out for plating to quantify the starting cell density, then cells were distributed into 96-well round-bottom clear polypropylene plates (Corning) to a final volume of 100 μL with antibiotic. Plates were sealed using AeraSeal membranes (Sigma-Aldrich) and incubated for three hours at 37°C with 900 r.p.m. shaking. Next, plates were centrifuged for seven minutes at 4000 x g at 4°C, then resuspended in an equal volume of PBS to remove antibiotic. Cells were serially diluted 10-fold

in PBS, spotted on LB agar plates, and incubated overnight at 37°C. In cases where the number of CFUs was below this limit of detection, the entire undiluted well volume (100 μL) was spread on LB agar for counting. Log survival (as in Figures 1G–1K and S2B) was determined by dividing the CFU/mL viability after three-hour antibiotic treatment by the starting CFU/mL prior to antibiotic treatment to obtain % survival. This value was then log-transformed to obtain log survival.

Effect of L-cysteine Addition

Cells were grown as described above for varied nutrient conditions, except 1 mM L-cysteine or 1 mM L-alanine was added during the two-hour incubation period in 10% or 1% LB. Cultures were then back-diluted to ~10^6 CFU/mL in the same media containing either 1 mM L-cysteine or 1 mM L-alanine, and treated with gentamicin or kanamycin as described above for three hours.

Quantification of ATP Levels

Cells were grown as described above for varied nutrient levels, except directly after the two-hour incubation period, cells were centrifuged at 4000 x g at room temperature for four minutes and re-suspended in an equal volume of PBS to remove differential media effects from the luminescence-based ATP assay. At this point, OD_{600} was measured using a Spectramax M3 plate reader (Molecular Devices) with 100 μL volume in a 96-well clear polypropylene plate (Corning). Next, ATP was measured using the BacTiter Glo assay kit (Promega) in a white opaque 96-well plate (Corning), according to the manufacturer's instructions. A standard curve was created using 10-fold dilutions of purified ATP in PBS and utilized to calculate the micromolar ATP concentration within bacterial samples, which was then normalized by OD_{600}. Luminescence was recorded in technical triplicate.

Determination of Metabolism Dependence

For each antibiotic, a linear regression was performed at each antibiotic concentration for data in Figures 1G–1K and S2B, with 10 points per regression. Slopes were then multiplied by -1, such that greater positive values indicate a higher metabolic dependence, and averaged across concentrations. All linear regressions were performed using GraphPad Prism 8.

Bacteriostatic Pre-treatment

E. coli BW25113 was grown overnight in 3 mL of LB at 37°C with 300 r.p.m. shaking, then diluted 1 in 10,000 into 25 mL of LB. This subculture was grown for 2.5 hours at 37°C with 300 r.p.m. shaking to OD_{600} 0.01, then distributed into 96-well plates. Chloramphenicol (20 μg/mL) or a vehicle (ethanol) control was added for 30 minutes prior to addition of bactericidal drugs for three hours. Plates were incubated at 37°C with 900 r.p.m. shaking, then centrifuged at 4000 x g at 4°C to remove antibiotic. Cells were serially diluted 10-fold in sterile PBS and 7 μL was plated on LB agar for counting, except in conditions where survival was below this limit of detection and thus the whole undiluted well volume was spread and counted.

Time-Kill Curves

Colonies of *E. coli* BW25113 were picked into 3 mL of LB and grown overnight at 37°C with 300 r.p.m. shaking. Subcultures were initiated by diluting overnight cultures 1 in 10,000 into 25 mL of LB and incubating for 2.5 hours at 37°C with 300 r.p.m. shaking until the OD_{600} reached 0.01. Cells were then distributed into 96-well plates, antibiotic was added, and plates were sealed and incubated at 37°C with 900 r.p.m. shaking. Plates were taken out at 0, 1, 2, 3, and 6 hours after antibiotic addition to assess survival. For CFU counting, plates were centrifuged at 4000x g at 4°C to remove antibiotic, then serially diluted 10-fold in sterile PBS. 7 μL was spotted on LB agar, or the whole well volume was spread where necessary to improve the limit of detection.

Density Dependence of WDM Antibiotics

Cultures of *E. coli* BW25113 were grown overnight in 3 mL of LB at 37°C with 300 r.p.m. shaking, then serially diluted 10-fold in fresh LB to create a gradient of culture densities ranging from 10^3 to 10^9 CFU/mL. Cells were then distributed into 96-well plates with two-fold dilutions of antibiotics and incubated at 37°C with 900 r.p.m. shaking for three hours. Plates were centrifuged at 4000 x g and 4°C then serially diluted in sterile PBS. 7 μL was spotted on LB agar for counting, except where cell counts were below this limit of detection and the entire well volume was spread.

Killing Checkerboards

For killing checkerboards, overnight cultures of *E. coli* BW25113 were grown in 3 mL of LB at 37°C with 300 r.p.m. shaking. Overnight cultures were then diluted 1 in 10,000 into 25 mL of LB and grown for 2.5 hours at 37°C with 300 r.p.m. shaking to OD_{600} 0.01, then distributed into 96-well plates. Antibiotics were serially diluted two-fold, and the first antibiotic was added for three hours; then the second antibiotic was added for another three hours to create a checkerboard array of concentrations. Antibiotic treatment was conducted at 37°C with 900 r.p.m. shaking. Following treatment, plates were centrifuged at 4000x g and 4°C to remove antibiotic, then cells were serially diluted 10-fold in sterile PBS. 7 μL was then spotted on LB agar, except for where cell counts were below this limit of detection and the whole undiluted well volume was spread. At least two biological replicates were conducted for each killing checkerboard, and the means for each condition were taken. Individual replicates of killing checkerboards are shown in Figure S3. In all killing checkerboard representations, the first antibiotic added is depicted on the vertical axis, and the second antibiotic added is

on the horizontal axis. For kinetic analysis, plates were taken out every hour after antibiotic addition for serial dilution and plating. For simultaneous killing checkerboards, both antibiotics were added together for three hours directly after the 2.5-hour subculture, then survival was evaluated.

Growth-Inhibition Checkerboards and MIC

Overnight cultures of *E. coli* BW25113 were grown in 3 mL of LB, then diluted 1 in 10,000 into fresh LB and distributed into 96-well plates with two-fold serial dilutions of indicated antibiotic(s) in a final volume of 100 μL. Plates were incubated for 24 hours at 37°C with 900 r.p.m. shaking, then read at OD_{600} on a Spectramax M3 plate reader. For checkerboards, the FICI was calculated as

$$FICI = \frac{MIC_{AB}}{MIC_A} + \frac{MIC_{BA}}{MIC_B}$$

where MIC_A is the MIC of drug A alone, MIC_B is the MIC of drug B alone, MIC_{AB} is the MIC of drug A in combination with drug B, and MIC_{BA} is the MIC of drug B in combination with drug A. An FICI of ≤ 0.5 is indicative of synergy, and ≥ 4 indicates antagonism. Values in between 0.5 and 4 indicate no interaction. Three biological replicates were conducted for each checkerboard, and the mean values were used in calculating the FICI. Individual checkerboard replicates are shown in Figure S4.

QUANTIFICATION AND STATISTICAL ANALYSIS

The number of biological replicates and meaning of error bars can be found in the figure legends or in the upper right corner of checkerboards. Graphpad Prism 8 was used to perform linear regressions of data in Figures 1G–1K and S2B, with 10 points per regression. Linear regression statistics (slope and R^2) are shown in Table S1.